


Contents lists available at ScienceDirect

Earth and Planetary Science Letters

www.elsevier.com/locate/epslThe elastic properties of hcp-Fe_{1-x}Si_x at Earth's inner-core conditions Benjamí Martorell ^{*},¹, Ian G. Wood, John Brodholt, Lidunka Vočadlo

Department of Earth Sciences, University College London, Gower Street, London, WC1E 6BT, United Kingdom

ARTICLE INFO

Article history:

Received 24 January 2016
Received in revised form 27 June 2016
Accepted 11 July 2016
Available online 26 July 2016
Editor: C. Sotin

Keywords:

iron–silicon alloys
Earth's inner core
seismic wave velocities
ab initio simulations
molecular dynamics
elastic properties

ABSTRACT

The density of the Earth's inner core is less than that of pure iron and the P-wave velocities and, particularly, the S-wave velocities in the inner core observed from seismology are lower than those generally obtained from mineral physics. On the basis of measurements of compressional sound velocities to ~100 GPa in diamond-anvil cells, extrapolated to inner-core pressures, it has been suggested that both the inner-core density and P-wave velocity can be matched simultaneously by the properties of a hexagonal-close-packed (hcp) Fe–Si or Fe–Ni–Si alloy. In this paper we present the results of *ab initio* molecular dynamics simulations of hcp-Fe–Si alloys at 360 GPa and at temperatures up to melting. We find that although the inner-core density can be readily matched by an Fe–Si alloy, the same is not true for the wave velocities. At inner-core temperatures, the P-wave velocity in hcp-Fe–Si remains equal to, or slightly above, that of hcp-Fe and shows little change with silicon content. The S-wave velocity is reduced with respect to that of pure hcp-iron, except for temperatures immediately prior to melting, where the velocities are almost equal; this is a consequence of the fact that the strong temperature dependence of the shear modulus that was seen in similar simulations of hcp-Fe just prior to melting was not found in hcp-Fe–Si, and so in this temperature range the reduced S-wave velocity of pure iron closely matches that of the alloy. Our results show that for an hcp-Fe–Si alloy matching the inner-core density, both the P-wave and the S-wave velocities will be higher than those observed by seismology and we conclude, therefore, that our calculations indicate that inner core velocities cannot be explained by an hcp-Fe–Si alloy. The opposite conclusion, obtained previously from experimental data measured at lower pressures, is a consequence of: (i) the necessarily large extrapolation in pressure and temperature required to extend the experimental results to inner-core conditions and (ii) the use of a velocity–density relationship for pure hcp-iron that is now considered to be incorrect.

© 2016 The Authors. Published by Elsevier B.V. This is an open access article under the CC BY license (<http://creativecommons.org/licenses/by/4.0/>).

1. Introduction

Direct observations of the Earth's core are made through seismic waves, whose velocities are dependent on the elastic properties of the material present. For the outer-core, the seismic observations are consistent with iron alloyed with light elements, albeit with uncertainty over the exact composition (e.g. [Badro et al., 2014](#)). For the inner core, however, things are far less certain. P-wave velocities and, in particular, S-wave velocities are observed to be much lower (10–30%) than those generally inferred from mineral physics (e.g. [Vočadlo, 2007](#)), and increasingly accu-

rate seismic observations have shown the Earth's inner core to be far more complex than had previously been thought (e.g. [Tkalcíć, 2015](#)). Current seismological models reveal an inner core that is anisotropic, layered and laterally heterogeneous, but the origins of these characteristics are not yet fully understood (see e.g., [Wang et al., 2015](#)). Interpretation of the increasingly detailed seismic data for the inner core must ultimately depend on accurate knowledge of the elastic properties of the constituent materials, but the exact composition of the inner core remains unknown and so a number of candidates must be considered. It has been supposed for many years that the inner-core density is less than that of pure iron and, therefore, that one or more light alloying elements must be present ([Birch, 1952](#); [Alfè et al., 2007](#); [Hirose et al., 2013](#); [Deng et al., 2013](#)). One of the more likely candidate elements is silicon – geochemical models based on cosmochemical arguments suggest that Earth's core could contain up to 20 wt.% Si (see e.g. [Fischer et al., 2012](#)).

A number of experimental studies of Fe–Si alloys have now been reported. The phase relations in the Fe–Si system have

^{*} Author contributions: L.V., I.G.W. designed research; B.M. performed research; B.M., J.B., I.G.W. and L.V. analysed data; B.M., J.B., I.G.W. and L.V. wrote the paper.

^{*} Corresponding author.

E-mail address: b.massip@ucl.ac.uk (B. Martorell).

¹ Now at: Derogallera LTD, Dpt. Materials Science, De Clare Court, Pontigwindy Industrial State, Caerphilly, CF83 3HU, Wales, United Kingdom.

been studied using laser-heated diamond-anvil cells combined with either *in situ* high- P/T X-ray diffraction or post analysis of quenched samples. On the basis of quenching experiments, Lin et al. (2003a) concluded that $\text{Fe}_{0.85}\text{Si}_{0.15}$ adopts the hexagonal-close-packed (hcp) structure above 36 GPa. *In situ* studies of alloys containing between 3.4 and 16 wt.% Si, extending to 250 GPa and 4000 K (Asanuma et al., 2008; Kuwayama et al., 2009; Fischer et al., 2012, 2013), have also all indicated that the Fe–Si alloy adopts the hcp structure at high pressure. There is, however, some uncertainty between these different studies as to the maximum solubility of silicon in iron under core conditions and, therefore, as to whether the alloy exists as a single hcp phase or whether it occurs in coexistence with CsCl-structured stoichiometric FeSi. Equation-of-state measurements of Fe–Si alloys have been used to estimate the possible Si content of the core giving values of 3–5 wt.% (Hirao et al., 2004), 4–6 wt.% (Asanuma et al., 2011; assuming also 4–5 wt.% Ni) and 4–9 wt.% (Fischer et al., 2014).

The extent to which the melting curve of iron is lowered by the inclusion of Si (or other alloying elements) is crucial to our understanding of core formation as the melting temperature defines the inner core boundary. Recent experimental studies suggest that the effect of Si on the melting temperature at core pressures may be very small, perhaps only of the order of 100 K, and that the percentage of silicon at the eutectic decreases with pressure, from ~15 wt.% at ambient pressure (Davies et al., 2002) to ~6 wt.% at 145 GPa (Fischer et al., 2013).

Given the importance of matching seismic observations, measurements of sound velocities in core-forming phases (Badro et al., 2007) give what is probably the most direct test of candidate materials. Sound velocity–density measurements for hcp-Fe–Si and hcp-Fe–Ni–Si alloys have shown that, for a given density, the presence of Si increases V_P (Lin et al., 2003b; Antonangeli et al., 2010; Mao et al., 2012). Lin et al. (2003b) also found that V_S increased with Si content (again at constant density). When considering these results, it should be noted, however, that at constant pressure, rather than at constant density, the situation may be reversed, with both density and sound velocities in the Fe–Si alloy decreasing with increasing Si content. By extrapolation of their measurements (made at pressures up to 68 GPa and 98 GPa respectively) to inner-core pressures, Antonangeli et al. (2010) and Mao et al. (2012) concluded that a match could be obtained to both the wave velocities and densities in the inner core on the basis of an hcp Fe–Ni–Si alloy (Antonangeli et al., 2010) or an hcp Fe–Si alloy (Mao et al., 2012).

However, although many of the experimental studies on Fe–Si alloys discussed above represent the current state-of-the-art, in some cases reaching extremely high pressures and temperatures, inner-core conditions have yet to be achieved. Whether the results of such experiments can then be safely extrapolated to the inner core is not certain, as it cannot be assumed *a priori* that the properties of such alloys will not change at higher pressures and temperatures, especially at temperatures very close to melting, which is the temperature regime for the whole of the inner core. In contrast, computer simulations can, in principle, directly access the entire range of P/T space in the core, and so they may, therefore, be the best method currently available to determine the relevant properties of the constituent materials. Previous *ab initio* computational studies of hcp-Fe–Si alloys as a function of pressure at zero Kelvin have been made by Côté et al. (2008) and by Tsuchiya and Fujibuchi (2009). In both cases it was found that, although the hcp-structured phase remained the most stable form at inner-core pressures, the addition of silicon to iron stabilised the body-centred-cubic (bcc) structure relative to the hcp structure, leading Côté et al. (2008) to suggest that the bcc phase might become thermally stabilised in the inner core. Tsuchiya and Fujibuchi (2009) also investigated the effect of silicon on the elastic con-

stants, finding that, although it decreased the shear modulus of the hcp phase, cancellation of the changes in density and elastic moduli meant that it did not drastically change the elastic wave velocities from those of iron. Côté et al. (2010) carried out a further *ab initio* study of Fe–Si alloys, extending it to high temperatures by means of lattice dynamics. They found that for ~7 wt.% silicon, the combination of temperatures over 4000 K and light element enrichment acted to make the face-centred-cubic (fcc) phase thermodynamically stable at core conditions, while the hcp structure remained the stable phase at lower pressures and temperatures. This led to the suggestion that the inner core might lie in the two-phase region of the Fe–Si phase diagram, with fcc and hcp structures coexisting. However, as the temperatures throughout the inner core are very close to melting, anharmonicity in the atomic vibrations is expected to be large and, therefore, results based on lattice dynamics should probably be treated with some caution.

In recent papers, we have used *ab initio* molecular dynamics to calculate the effect of temperature on the elastic properties of hcp-Fe at 360 GPa (Martorell et al., 2013a, 2015). We observed that, after a linear decrease in both V_P and V_S with temperature, a significant pre-melting effect occurred close to melting, reducing the shear modulus and giving, as a result, a much lower V_S than would be expected by extrapolation from the linear region at lower temperatures. The reduction in wave velocities was sufficient to match the values obtained by seismology for the Earth's inner core, as given in PREM (Dziewonski and Anderson, 1981); however, the densities obtained from the simulations, even at very high temperature (7000 K) were still too high and so the requirement for a light alloying element remains. To determine whether similar pre-melting effects might also occur in Fe–X alloys as opposed to pure hcp-Fe, in this paper we report, therefore, a study of the density and elastic properties of hcp-Fe–Si alloys at Earth's inner-core conditions using first-principles calculations. We have not included Ni in these simulations as in our previous work we demonstrated that Ni does not significantly affect the density and elastic properties of iron at core temperatures (Martorell et al., 2013b, 2015). Our *ab initio* molecular dynamics simulations were performed at 360 GPa and temperatures up to melting on hcp-Fe–Si alloys with 3.25 wt.% Si (6.25 atm.%) and 6.70 wt.% Si (12.5 atm.%).

2. Methods

2.1. Electronic structure calculations

The calculations performed in this work are based on density functional theory (DFT) using the Vienna Ab Initio Simulation Package (VASP: Kresse and Hafner, 1993a, 1993b, 1994). To solve the Kohn–Sham equations, this code makes use of a development of the one-electron wave function in a basis of plane waves. The effect of the core electrons on the valence electrons is described by the projector augmented wave method (PAW: Blöchl, 1994; Kresse and Joubert, 1999). The generalised gradient approximation (GGA) was used with the functional of Perdew and Wang (1992). A convergence of the plane-wave expansion was obtained with a cut-off of 400 eV.

We ran finite temperature *ab initio* molecular dynamics (AIMD). The VASP code uses the Verlet algorithm to integrate the classical Newton's equations of motion. A time step of 1.5 fs was used for the integration. Simulations were performed at constant temperature using an Andersen thermostat, with a restarting value of 150 cycles.

The simulation box for the hcp- $\text{Fe}_{0.9375}\text{Si}_{0.0625}$ (3.24 wt.% Si) and hcp- $\text{Fe}_{0.875}\text{Si}_{0.125}$ (6.70 wt.% Si) calculations was the same as used previously (Vočadlo et al., 2009; Martorell et al., 2013a, 2013b) to determine the elastic constants of pure hcp-Fe iron. This

consisted of a $4 \times 2 \times 2$ supercell of the 4-atom C-centred crystallographic cell of the hcp structure with orthogonal axes. For hcp-Fe_{0.9375}Si_{0.0625}, four Fe atoms in this structure were systematically substituted by Si atoms, in the most dispersed way possible (the most energetically favourable of ten separate configurations that were tested). For hcp-Fe_{0.875}Si_{0.125}, eight Fe atoms were, once again, systematically substituted by Si atoms, in the most dispersed way possible. A k -points grid of 4 irreducible k -points was used; the resulting stresses are insensitive to a denser k -point grid.

Simulations were performed at nominal temperatures of 0, 2000, 4000, 5500, 6500, 7000, 7200, 7350, 7500 and 7600 K for hcp-Fe_{0.9375}Si_{0.0625} and at 0, 5500, and 6500 K for hcp-Fe_{0.875}Si_{0.125}. Simulations were run for between 10 and 15 ps. The actual temperature of the simulation was determined from an average excluding the first 2 ps of the simulation. Stresses were determined as outlined below. To ensure that we were computing the stresses of solid phases, we retrieved the mean square displacements (MSD) for the last 10 ps of each simulation.

2.2. Elastic properties

In order to obtain the elastic properties at 360 GPa we used the same procedure as before (Martorell et al., 2013a, 2013b). In summary, we first optimised the unit-cell parameters and densities using VASP-NPT simulations for the isothermal–isobaric ensemble using the barostat implemented in VASP by Hernández (Hernández, 2001); we ran this simulation for up to 5 ps. The average lattice parameters from these NPT simulations were then used to create a unit cell to which distortions were applied (see below); the stresses on the simulation box were then obtained from VASP-NVT simulations run over ~ 10 ps (for simulations at target temperatures beyond 7000 K, 15 ps were used to ensure convergence).

Once the equilibrium structure of each system was obtained, the elastic constants, c_{ij} , were evaluated by distorting the unit cells according to the two distortion matrices shown below:

$$\begin{pmatrix} 1 + \delta & 0 & 0 \\ 0 & \sqrt{3} & \delta\sqrt{3} \\ 0 & \delta(\frac{c}{a}) & (\frac{c}{a}) \end{pmatrix} \text{ and } \begin{pmatrix} 1 & 0 & 0 \\ 0 & \sqrt{3} & 0 \\ 0 & 0 & (\frac{c}{a})(1 + \delta) \end{pmatrix}$$

We applied strain (δ) values of ± 0.01 and ± 0.02 . Within the Voigt average the elastic properties (incompressibility: K ; shear modulus: G) are given by:

$$K_T = \frac{2(c_{11} + c_{12}) + 4c_{13} + c_{33}}{9};$$

$$G = \frac{12c_{44} + 7c_{11} - 5c_{12} + 2c_{33} - 4c_{13}}{30}$$

Finally, we obtained the adiabatic incompressibility, K_S , from the relation

$$K_S = K_T(1 + \alpha\gamma T)$$

using values of the volumetric thermal expansion coefficient, $\alpha = 10^{-5} \text{ K}^{-1}$ and the Grüneisen parameter, $\gamma = 1.5$ (Vočadlo et al., 2003; Vočadlo, 2007). The isotropic wave propagation velocities in the material can then be evaluated from the bulk and shear moduli, and the density, ρ , as follows:

$$V_P = \sqrt{\frac{K + \frac{4}{3}G}{\rho}}; \quad V_S = \sqrt{\frac{G}{\rho}}$$

The maximum anisotropy (A) in V_P , defined here as the percentage difference in velocities between the fastest and slowest directions in the crystal, has also been evaluated using the Petrophysics software developed by Mainprice (1990).

Before presenting the results of our simulations, it is necessary to comment on two aspects of our methodology. Firstly, the procedure described above for deriving the elastic moduli assumes that the material has hexagonal symmetry; strictly, this assumption is incorrect as some of the Fe atoms have been replaced by silicon. The magnitude of the effect of the broken symmetry on the resulting elastic moduli can be assessed by examination of the stress matrices for the simulations at zero K. These showed that the deviations from the expected form (e.g. hexagonal symmetry requires $\sigma_5 = \sigma_6 = 0$ for both distortion matrices) were sufficiently small, being < 0.01 GPa, that they could be considered insignificant in comparison to the inevitable random fluctuations in the stresses on the simulation box at high temperatures (~ 1 GPa) which are inherent in MD simulations run over a time period of only a few picoseconds. Secondly, some consideration must be given to the range of temperature over which the results may be considered fully reliable. For pure iron, the results of Alfè (2009), obtained from MD simulations in which solid and liquid were seen to co-exist, indicate that at 360 GPa melting should occur at ~ 6600 K. Since our simulation methodology is essentially the same as that employed by Alfè (2009), and given that the introduction of the Si atoms seems to have little effect on the melting point (see below) we can, therefore, consider all of our results up to this temperature to be reliable. However, at higher temperatures it is possible that the results from the simulations represent the properties of a super-heated solid, with melting suppressed by the lack of any free surface at which it can initiate. Nonetheless, although they should be treated with some caution, we believe that the simulations above 6600 K are of value as they enable us to estimate the relative melting temperatures of the Fe–Si alloys with respect to that of Fe and as they enable us to assess whether the elastic properties of the alloys show any increased temperature dependence just prior to melting.

3. Results

3.1. Density of hcp-Fe_{0.9375}Si_{0.0625} and hcp-Fe_{0.875}Si_{0.125} at 360 GPa

We have evaluated the densities of hcp-Fe_{0.9375}Si_{0.0625} at 360 GPa at 0, 2000, 4000, 5500, 6400, 6900, 7200, and 7350 K, and of hcp-Fe_{0.875}Si_{0.125} at 360 GPa and 0, 5500 and 6500 K. In Fig. 1 and Table 1 we present the evolution of the densities with temperature for the two alloys, together with that for pure hcp-Fe as calculated previously (Martorell et al., 2013a, 2015). For comparison we have also added the PREM value at this pressure (Dziewonski and Anderson, 1981). We observe that, for hcp-Fe_{0.9375}Si_{0.0625}, the reduction in density, with respect to that of pure iron, is almost constant over the entire temperature range, being $\sim 390\text{--}460 \text{ kg m}^{-3}$ ($\sim 2.9\text{--}3.4\%$) throughout, and that the density of hcp-Fe_{0.9375}Si_{0.0625} is in good agreement with PREM for simulation temperatures above ~ 6900 K. At zero K, the reduction in density for hcp-Fe_{0.875}Si_{0.125} with respect to pure iron is almost exactly twice that for hcp-Fe_{0.9375}Si_{0.0625}, suggesting a linear relationship between density and Si content. However, at 5500 K and 6500 K the density reduction is larger than would be expected from the zero K results on a linear basis, and this non-linearity seems to increase with temperature. Thus, a density match with PREM for this composition would be achieved at a much lower simulation temperature of ~ 4000 K. Clearly, depending upon the temperature chosen, the inner-core density can be matched by that of hcp-Fe–Si alloys in the composition range considered here, but the non-linearity of density reduction with Si content makes it more difficult to simply fit the actual core density to the density of the binary hcp-Fe–Si alloy as a function of temperature and Si concentration.

Table 1Elastic properties and densities for hcp-Fe, hcp-Fe_{0.9375}Si_{0.0625} and hcp-Fe_{0.875}Si_{0.125} alloy and PREM at 360 GPa. A is maximum anisotropy in % for V_p .

	T_{Final} (K)	ρ (kg m ⁻³)	c_{11} (GPa)	c_{12}	c_{33}	c_{13}	c_{44}	K_S (GPa)	G	V_p (km s ⁻¹)	V_s	A
Fe ^a	0	14 185	2493	1151	2689	1085	577	1590	655	13.18	6.80	5.7
	2000	14 138	2356	1282	2571	1083	476	1622	554	12.92	6.26	7.0
	4000	13 880	2092	1292	2275	1063	351	1566	423	12.39	5.52	7.3
	5500	13 739	1942	1303	2097	1077	276	1546	341	12.07	4.98	7.1
	6600	13 628	1803	1297	2067	1132	232	1560	284	11.93	4.57	9.2
	7000	13 529	1708	1289	1890	1060	202	1489	250	11.60	4.29	7.7
	7250	13 495	1653	1384	1824	1046	151	1488	198	11.39	3.82	8.6
	7340	13 482	1579	1399	1786	1013	153	1454	180	11.21	3.65	9.2
Fe _{0.9375} Si _{0.0625}	0	13 733	2448	1265	2682	1065	501	1596	597	13.20	6.60	7.6
	2000	13 689	2288	1312	2518	1103	430	1617	508	12.95	6.09	7.5
	4000	13 489	2019	1319	2266	1094	325	1569	387	12.43	5.35	8.2
	5500	13 310	1897	1320	2046	1101	267	1550	319	12.18	4.89	6.5
	6400	13 164	1707	1353	1971	1112	191	1527	232	11.81	4.20	9.2
	6900	13 101	1674	1401	1855	1120	176	1531	202	11.72	3.93	7.2
	7200	13 096	1642	1375	1852	1127	167	1526	195	11.67	3.85	7.9
	7350	13 090	1620	1403	1901	1082	168	1514	193	11.64	3.84	9.2
Fe _{0.875} Si _{0.125}	0	13 310	2290	1315	2555	1085	392	1567	497	13.94	6.11	9.1
	5500	12 861	1833	1358	2002	1112	230	1543	279	12.20	4.66	7.1
	6500	12 626	1742	1397	1857	1031	172	1495	229	11.94	4.25	8.0
PREM ^b		13 090								11.26	3.67	

Errors are $\sim 2\%$ in c_{ij} and $\sim 1\%$ in V_p and V_s at 0 K, rising to 5% and 3% respectively at the very highest temperatures (Martorell et al., 2013b).

^a Martorell et al. (2013a).

^b Dziewonski and Anderson (1981).

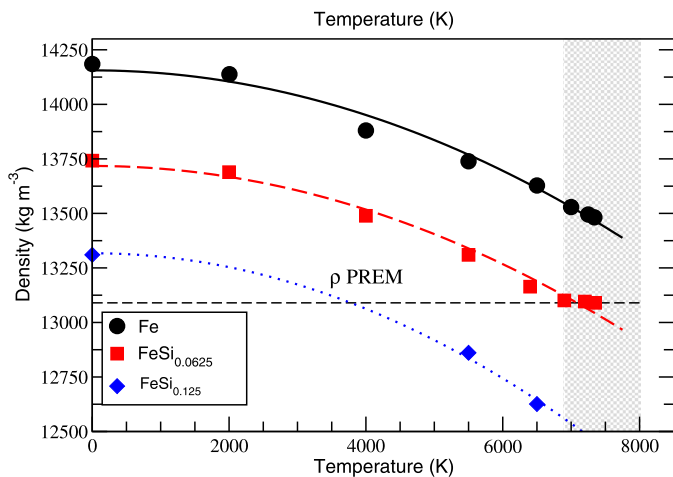


Fig. 1. Calculated densities for hcp-Fe (Martorell et al., 2013a, 2015), hcp-Fe_{0.9375}Si_{0.0625} and hcp-Fe_{0.875}Si_{0.125} as a function of simulation temperature at 360 GPa. The curves are just guides to the eye. The grey band represents the minimum and maximum melting temperatures presented in the paper of Morard et al. (2011; and the references therein) for hcp-Fe at 360 GPa.

3.2. Elastic properties of hcp-Fe_{0.9375}Si_{0.0625} and hcp-Fe_{0.875}Si_{0.125} at 360 GPa

The elastic constants of hcp-Fe_{0.9375}Si_{0.0625} and hcp-Fe_{0.875}Si_{0.125} as a function of temperature are shown in Table 1, together with those calculated previously for pure hcp-Fe (Martorell et al., 2013a, 2015). The elastic constants of the Fe–Si alloy have the same trend with T as pure hcp-Fe, but in general, the addition of Si in hcp-Fe makes the material softer with respect to the pure metal, i.e. c_{11} , c_{33} , and c_{44} decrease and c_{12} and c_{13} increase with respect to pure hcp-Fe. There is, however, an important difference in that at the last simulation point at 7350 K hcp-Fe_{0.9375}Si_{0.0625} shows systematically higher elastic constants than pure hcp-Fe; the origin of this effect would appear to be that in hcp-Fe_{0.9375}Si_{0.0625} there is no indication of the significant reduction of the elastic constants that was found in pure iron, which was attributed to premelting behaviour (Martorell et al., 2013a).

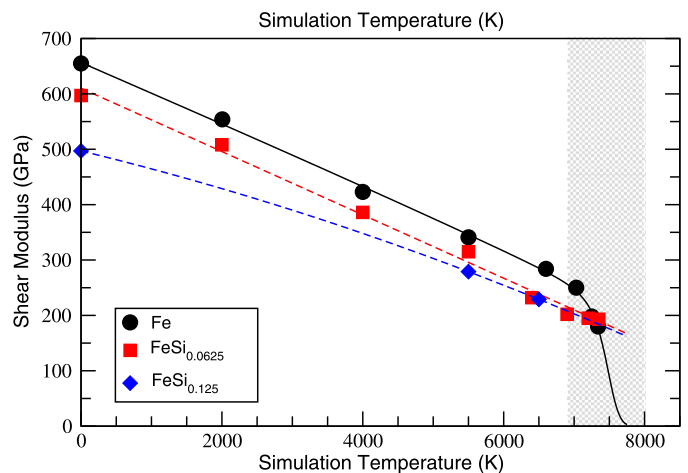


Fig. 2. Calculated shear modulus for hcp-Fe (Martorell et al., 2013a, 2015), hcp-Fe_{0.9375}Si_{0.0625} and hcp-Fe_{0.875}Si_{0.125} as a function of simulation temperature at 360 GPa. The hcp-Fe curve is fitted to an NP-like model (Martorell et al., 2013a, 2015). The curves shown for the hcp-Fe–Si alloys are merely guides to the eye. The grey band represents the minimum and maximum melting temperatures presented in the paper of Morard et al. (2011; and the references therein) for hcp-Fe at 360 GPa.

Table 1 also shows the calculated adiabatic bulk modulus (K_S) and shear modulus (G). Up to 5500 K, K_S is almost unaffected by the addition of Si. At ~ 6500 K there is possibly a slight reduction in K_S , relative to that of hcp-Fe, by $\sim 2\%$ and $\sim 4\%$ for hcp-Fe_{0.9375}Si_{0.0625} and hcp-Fe_{0.875}Si_{0.125} respectively. However, at the highest temperatures (>6500 K), K_S for hcp-Fe_{0.9375}Si_{0.0625} is slightly higher than the corresponding value for pure iron (by 2–4%), again possibly due to the absence of any premelting behaviour. The shear modulus, G , however, behaves differently (Fig. 2). For hcp-Fe two different zones exist in $G(T)$: i) <7000 K a nearly linear decrease in G as a function of temperature occurs; ii) >7000 K a strong pre-melting effect is observed, where G drops much more rapidly than in the linear region, just before the melting point. This behaviour was fitted using a Nadal–Le Poac model (Nadal and Le Poac, 2003), from which we obtained a melting tem-

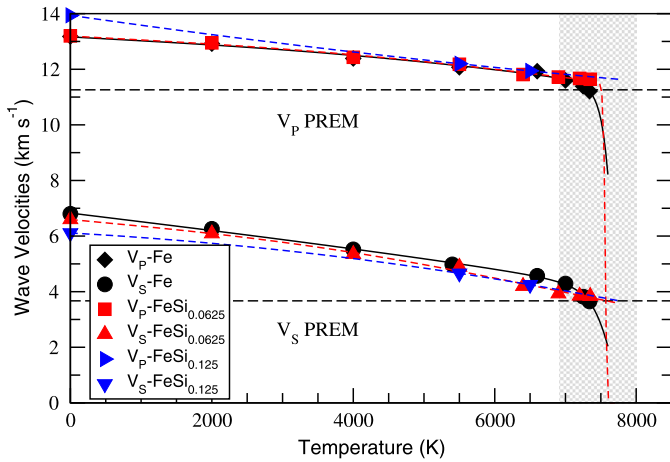


Fig. 3. Calculated compressional and shear wave velocities for hcp-Fe (Martorell et al., 2013a, 2015), hcp-Fe_{0.9375}Si_{0.0625} and hcp-Fe_{0.875}Si_{0.125} as a function of simulation temperature at 360 GPa. The curves are fits to NP-like models. The grey band represents the minimum and maximum melting temperatures presented in the paper of Morard et al. (2011; and the references therein) for hcp-Fe at 360 GPa.

perature for pure hcp-Fe of ~ 7350 K (Martorell et al., 2013a). In this work, for hcp-Fe_{0.9375}Si_{0.0625} below 7000 K we also observe nearly linear behaviour, with the same slope as for hcp-Fe but displaced by ~ 50 GPa below the hcp-Fe line; above 7000 K the linear behaviour continues, and no large drop in G is observed before melting. For hcp-Fe_{0.875}Si_{0.125}, a much greater reduction in G is observed at zero K, but as the temperature increases, G approaches that of hcp-Fe_{0.9375}Si_{0.0625} with the values for the two alloys becoming equal at ~ 6500 K.

Studies of the behaviour of G as a function of temperature very close to melting are limited in the literature, being constrained to pure elements such as Sn (Nadal et al., 2009) or Mo (Nguyen et al., 2014). This makes interpretation of the results for multi-component systems more difficult because we cannot compare our finding of the lack of a pre-melting effect in hcp-Fe_{0.9375}Si_{0.0625} with the behaviour of other two or three component materials. More studies of G close to the melting point, for both pure, as well as multicomponent systems are required. Our results for hcp-Fe_{0.9375}Si_{0.0625} clearly show that pre-melting behaviour is not observed, and therefore the reduction in G immediately prior to melting must be even more discontinuous in the alloy.

Fig. 3 and Table 1 show V_P and V_S for pure hcp-Fe and for our two alloys. At zero K, V_P for hcp-Fe_{0.875}Si_{0.125} is about 6% higher than for either hcp-Fe or hcp-Fe_{0.9375}Si_{0.0625}, but at higher temperatures the effect of Si is reduced to the extent that the values of V_P in the temperature range from 5500–7000 K are unaffected by silicon content. For simulation temperatures above 7000 K, due to the absence of any pre-melting effect, hcp-Fe_{0.9375}Si_{0.0625} has a higher V_P than pure hcp-Fe (by $\sim 4\%$). The effect of Si on V_S is similar to its effect on the shear modulus. At zero K, both alloys show a reduction in V_S with respect to that for hcp-Fe, with the reduction being more pronounced for Fe_{0.875}Si_{0.125}. At 5500 K and 6500 K, however, the values of V_S for the two alloys are very similar, indicating that V_S cannot be reduced simply by an increase in silicon content. With respect to hcp-Fe, below 7000 K, V_S for hcp-Fe_{0.9375}Si_{0.0625} is ~ 0.15 – 0.3 km s⁻¹ (3–9%) slower, but beyond that temperature, because no pre-melting effect is observed, the values of V_S for the alloy become very similar, and possibly slightly higher, than those for pure iron.

When considered together, the results shown in Fig. 1 and Fig. 3, suggest that it is quite difficult to match exactly the values of density, V_P and V_S for the centre of the inner core on the basis of an hcp-FeSi alloy. Clearly, for any chosen inner-core tem-

perature, a composition (probably fairly close to Fe_{0.9375}Si_{0.0625}) may be found that will produce the required density (Fig. 1), but Fig. 3 suggests that both V_P and V_S for such an alloy will only approach the PREM values if very high temperatures (probably above the true thermodynamic melting point) are allowed and that, even then, both velocities may well be higher than those of PREM by $\sim 3\%$ and $\sim 5\%$ respectively. Furthermore, Fig. 3 indicates that, in contrast to the resulting changes in density, varying the silicon content in the alloy does not lead to a range of velocities that bracket those from PREM, and so discrepancies in velocity with those from seismology cannot simply be resolved by varying the composition of the alloy.

3.3. Melting temperature of hcp-Fe_{0.9375}Si_{0.0625} relative to that of hcp-Fe

Since we have no free surfaces in the simulation box at which melting can initiate, absolute melting temperatures from our simulations are very likely to be overestimated; however, since the same ensemble of atoms was used in all cases, there is no reason to suppose that a reliable estimate of the relative melting temperatures cannot be obtained in this way. The last point that was simulated for solid Fe_{0.9375}Si_{0.0625} was at 7350 K, while a simulation at 7600 K completely melted. This limit of solid stability is similar to that found for pure hcp-Fe (Martorell et al., 2013a), suggesting that there is no significant reduction in melting temperature with Si content, in agreement with the conclusions of Fischer et al. (2013), based on laser-heated diamond-anvil-cell experiments, that silicon does not strongly depress the melting point of iron. A simulation of Fe_{0.9375}Si_{0.0625} at 7500 K gave results indicative of either enhanced diffusion of Si atoms or sub-lattice melting. At this temperature, the negative strains (-1 and -2%) led to a solid structure, but the positive ones (1 and 2%) made the system melt. For the non-strained system, the Si atoms were not stable in their initial positions, but exchanged with iron atoms, while the iron atoms themselves did not exchange with each other. The mobility of Si atoms in this simulation provides some evidence for enhanced diffusion, which could lead to chemical re-equilibration of the solid inner core and so have consequences for models of core structure and evolution (e.g. Yunker and Van Orman, 2007).

3.4. P-wave anisotropy

The compressional wave velocities in the inner core are quite strongly anisotropic, with velocities for waves travelling along the polar axis about 3–4% faster than for waves propagating in the equatorial plane (e.g. Souriau, 2007; Hirose et al., 2013). The origin of this effect is still not properly understood, but the most likely explanation is that it arises from a degree of preferred orientation in the crystals present. There is currently some debate as to whether the P-wave anisotropy in hcp-Fe at inner-core conditions is sufficient large to allow this interpretation. In previous studies of hcp-Fe we have found a maximum anisotropy (for non-perpendicular propagation directions) in the range 6–9% (Vočadlo et al., 2009; Martorell et al., 2013a), which might just be sufficient if the crystals were quite strongly oriented, but it has also been suggested that the anisotropy in hcp-Fe may be much smaller, $< 1\%$ (Sha and Cohen, 2010). The computed anisotropy in V_P for our simulations is presented in Table 1. Comparison of the results for hcp-Fe, hcp-Fe_{0.9375}Si_{0.0625} and hcp-Fe_{0.875}Si_{0.125} show they are very similar. In all of the calculations at finite temperature the addition of silicon changes the anisotropy by $\sim 1\%$ at most, although at zero K the effect is somewhat larger. It is clear, therefore, that the addition of Si does not significantly alter the anisotropy in V_P from that of hcp-Fe at the Earth's inner core conditions. For all

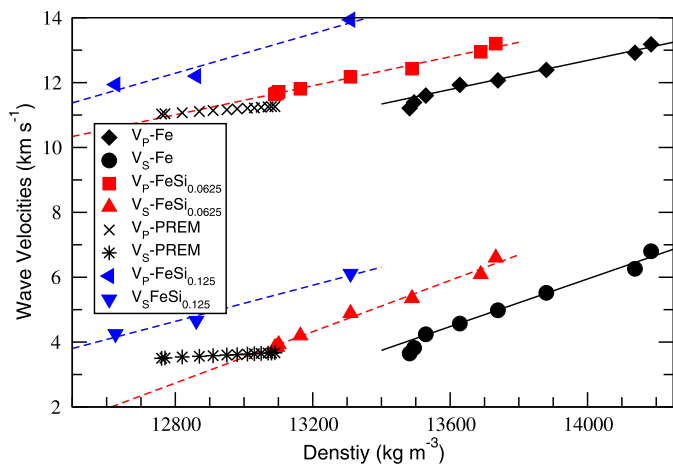


Fig. 4. Calculated compressional and shear wave velocities for hcp-Fe (Martorell et al., 2013a, 2015), hcp-Fe_{0.9375}Si_{0.0625} and hcp-Fe_{0.875}Si_{0.125} as a function of density at 360 GPa. The lines are linear fits to Birch's law. Values for the Earth's inner core from PREM are presented for comparison.

compositions there is possibly a slight increase in anisotropy with temperature, but the effect is not strong.

4. Discussion

4.1. Comparison with PREM

Fig. 4 shows the velocity versus density relationships from our simulations for hcp-Fe_{0.9375}Si_{0.0625} and hcp-Fe_{0.875}Si_{0.125}, as well as those from previous simulations on pure hcp-Fe (Martorell et al., 2013a, 2015), and those for the inner core from PREM (Dziewonski and Anderson, 1981). It can be seen that the three simulated systems, show linear behaviour of the velocities with respect to the density consistent with Birch's Law (only pure iron close to its melting point deviates from this trend). It should be noted, however, that since our simulations are isobaric, the changes in density arise solely from changes in temperature, whereas in the case of the values from PREM the density range arises very predominantly from the change in pressure, which may account for the differences in slope. When considering the agreement with the velocity data for the inner core, it can be seen from Fig. 4 (remembering that the simulations are at all 360 GPa, with the density changes due to temperature) that the values for hcp-Fe_{0.9375}Si_{0.0625} match those for the highest densities from PREM reasonably well only if simulation temperatures beyond 7000 K (i.e. probably above the thermodynamic melting temperature, as mentioned earlier) are allowed and that, even then, it is still the case that both V_P and V_S lie a little above the PREM values. Increasing the silicon content in the alloy would allow inner-core densities to be achieved at lower temperatures, but only at the cost of further increasing both V_P and V_S . It seems, therefore, that our simulations show that inner-core densities and velocities cannot be explained by an hcp-Fe–Si alloy.

4.2. Comparison with previous work

Since our results show that the wave velocities in the inner core are not consistent with the properties of an Fe–Si alloy, it is now worth considering why previous studies have come to the opposite conclusion. In general terms, the results of our simulations are in agreement with the experimental data on sound velocities in hcp-Fe–Si alloys measured at high pressure and room temperature, in that at constant density, both V_P and V_S increase with silicon content (Lin et al., 2003b; Antonangeli et al., 2010; Mao

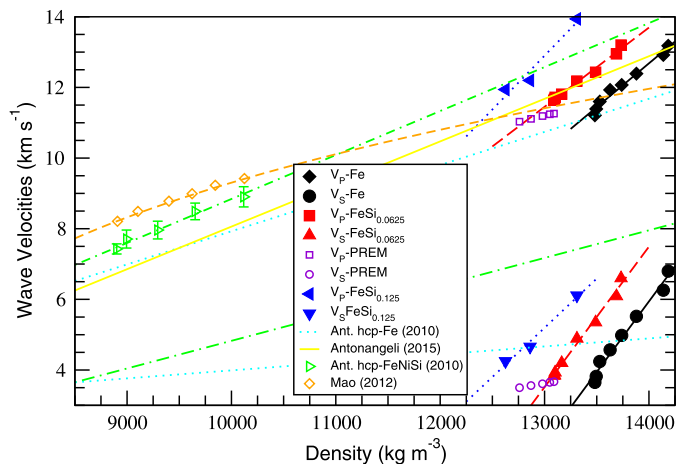


Fig. 5. Comparison of the simulated values of compressional and shear velocities for hcp-Fe (Martorell et al., 2013a, 2015), hcp-Fe_{0.9375}Si_{0.0625} and hcp-Fe_{0.875}Si_{0.125} as a function of density at 360 GPa, with the compressional wave velocities determined for hcp-Fe_{0.89}Ni_{0.04}Si_{0.07} by Antonangeli et al. (2010) and for hcp-Fe_{0.85}Si_{0.15} by Mao et al. (2012). Values for the Earth's inner core from PREM are also presented. The values from the present work (right-hand side of the diagram) are as shown in Fig. 4. The lower set of experimental data (5 points; green open triangles) are from Antonangeli et al. (2010; Fig. 3); the upper green dash-dotted line shows the weighted linear regression line fitted to these 5 data points. The dotted blue lines are the values for V_P and V_S for hcp-Fe given by Antonangeli et al. (2010; Fig. 3); the lower green dash-dotted line shows their values for V_S in hcp-Fe_{0.89}Ni_{0.04}Si_{0.07}. The upper set of experimental data (6 points; orange open diamonds) are from Mao et al. (2012); the orange dashed line is their power-law extrapolation. The solid yellow line shows the more recent relationship between V_P and density proposed by Antonangeli and Ohtani (2015). (For interpretation of the references to colour in this figure legend, the reader is referred to the web version of this article.)

et al., 2012). In Fig. 5 we compare our simulations to the experimental data of Antonangeli et al. (2010) for hcp-Fe_{0.89}Ni_{0.04}Si_{0.07} and of Mao et al. (2012) for hcp-Fe_{0.85}Si_{0.15}. Considering firstly the results of Antonangeli et al. (2010), we find that they are similar to our findings in as much as the addition of about 3.5 wt.% Si to hcp-Fe was found to increase V_P by ~ 900 m s⁻¹; however, although in both simulations and experiments linear relationships are seen relating V_P to density (with similar slopes for both the alloy and for hcp-Fe), the slopes of these lines are considerably steeper in our simulations (~ 2.2 m⁴ s⁻¹ kg⁻¹) than was found in the experiments (~ 1.1 m⁴ s⁻¹ kg⁻¹). For higher silicon content, our results for hcp-Fe_{0.875}Si_{0.125} agree somewhat less well with those of Mao et al. (2012), as we predict a larger change in V_P with respect to hcp-Fe. The slopes of the lines relating V_P and density found by Mao et al. (2012) are quite similar to those reported by Antonangeli et al. (2010), but Mao et al. (2012) also observed some curvature in the relationship for both hcp-Fe and hcp-Fe_{0.85}Si_{0.15}, which they found was better represented by an empirical power law than by a straight line. The gradient of the V_P vs density line from PREM (0.73 m⁴ s⁻¹ kg⁻¹) is shallower still than that found experimentally by both Antonangeli et al. (2010) and by Mao et al. (2012) for the lower-pressure region of their measurement range. Possible reasons for these differences in slope are that: (i) the effects of pressure and temperature on velocity are different and cannot both simply be subsumed, via the density, into Birch's law; (ii) the values from PREM for the inner core may reflect the suggestion that there is an inhomogeneous distribution of light elements whose concentration might change with depth (Labrosse, 2014). In either case it would appear that the general method of extrapolation based on Birch's law should be treated with some caution.

Experimental measurements of V_P at high pressures are still extremely challenging, and so must often be extrapolated over a wide range if they are to be used to determine velocities at inner-core densities. Nonetheless, Fig. 5 shows that there is almost

perfect agreement between the value of V_P for hcp-Fe_{0.9375}Si_{0.0625} from our 0 K *ab initio* simulations (the rightmost point on the figure) and the extrapolated value for hcp-Fe_{0.89}Ni_{0.04}Si_{0.07} from the experimental results of Antonangeli et al. (2010) at 300 K (especially when the difference in composition is taken into account). The different conclusion reached in our present study – that it will be difficult to match exactly the values of density, V_P and V_S for the centre of the inner core on the basis of an hcp-FeSi alloy – from that derived on the basis of their experiments by Antonangeli et al. (2010) – that such a match could be obtained with an hcp iron alloy containing 4–5 wt.% Ni + 1–2 wt.% Si – arises, therefore, not because our simulations differ from their experimental results for hcp-Fe–Ni–Si, but instead comes from the fact that the relationship between V_P and density that they assumed for *pure* hcp-Fe (the blue dotted line in Fig. 5) is now considered, by Antonangeli and Ohtani (2015), to be incorrect; very recently, Antonangeli and Ohtani (2015) have reviewed the available measurements for hcp-Fe and have concluded that (at 300 K) this relationship is best represented by $V_P = 1.206(11) \times 10^{-3} \rho - 4.00(11)$, where V_P is in km s⁻¹ and the density, ρ , is in kg m⁻³. This is shown in Fig. 5 by the solid yellow line, which once again we find to be in excellent agreement with the value from our 0 K computer simulation of pure hcp-Fe (Martorell et al., 2013a; 2013b; these simulated values of V_P for pure iron – 13.18 and 12.92 km s⁻¹ at 360 GPa and 0 and 2000 K respectively – are not only in excellent agreement with the value linearly extrapolated to 360 GPa from Antonangeli and Ohtani (2015) – 13.11 km s⁻¹ at 300 K, but also agree extremely well with the very recent experimental work of Sakamaki et al. (2016) – 13.02 and 12.96 km s⁻¹ at 300 and 2000 K respectively). On the basis of the older V_P -density relationship for hcp-Fe (which gave velocities lower than those from PREM) and their extrapolated values for hcp-Fe_{0.89}Ni_{0.04}Si_{0.07} (which gave velocities higher than those from PREM), and applying a small temperature correction, Antonangeli et al. (2010) were able to conclude that the PREM values could be matched by an alloy with an intermediate Si content. However, once the corrected relationship between V_P and density for hcp-Fe of Antonangeli and Ohtani (2015) is taken into account, it is immediately apparent that such a match can no longer easily be obtained in this way, as the velocities for hcp-Fe and hcp-Fe_{0.89}Ni_{0.04}Si_{0.07} are now both higher than those of PREM. Thus, despite the apparent contradiction in our conclusions, we consider that our results and those of Antonangeli et al. (2010) actually show very good agreement.

On the basis of a similar extrapolation of experimental measurements of sound velocities in hcp-Fe_{0.85}Si_{0.15} as a function of density, Mao et al. (2012) concluded that a match to the inner core could be obtained on the basis of an hcp iron alloy containing 8 wt.% Si. In this case, however, a power law extrapolation was used, which took the form $V_P = C(M)[\rho + a(T)]^\lambda$ (as shown in Fig. 5); this required three variable parameters, one of which, λ , was fixed at the value previously determined for hcp-Fe. In their review of the available experimental data for hcp-Fe, Antonangeli and Ohtani (2015) pointed out that the measurements of Mao et al. (2012) for hcp-Fe are the only ones suggesting a sub-linear dependence of V_P on density – all other determinations indicate a linear relationship (at 300 K) – and they suggest reasons why this non-linearity might be an artefact of the experimental method used. If a linear relationship between V_P and density is used to extrapolate the measurements of Mao et al. (2012), values of V_P that are 0.80–0.95 km s⁻¹ higher than those given by their power law are obtained at inner-core densities. Taking account of the large extrapolation range, the questions raised recently by Antonangeli and Ohtani (2015) as to the experimental methodology, and the applicability of the power law used for the extrapolation, we consider, therefore, that the conclusions of Mao et al. (2012) should probably be treated with some caution.

It would appear, therefore, that the results of our simulations are in excellent agreement with the experimental data of Antonangeli et al. (2010) and are in satisfactory agreement with those of Mao et al. (2012) if a linear extrapolation (as opposed to a power-law extrapolation) is used. As the experimental results place no constraints on our *ab initio* simulations, which directly access inner-core conditions, we believe, therefore, that there are good grounds for considering these simulations to be the more reliable method for determining the properties of the materials.

5. Summary and conclusions

We have used *ab initio* molecular dynamics to compute the densities and elastic properties of hcp-Fe–Si alloys at Earth's inner core conditions. In contrast to our previous simulations of hcp-Fe, we did not observe any strong reduction in the shear modulus at temperatures just below melting. We have found that these hcp-Fe–Si alloys cover a density range extending above and below that observed in the inner core and that the inner-core density can be matched by an alloy with a composition fairly close to hcp-Fe_{0.9375}Si_{0.0625} (with the exact composition required – probably a little richer in Si – depending upon the inner-core temperature). At very high simulation temperatures (>7000 K and so probably above the thermodynamic melting point) the density, P-wave and S-wave velocities of hcp-Fe_{0.9375}Si_{0.0625} approach those observed in the inner core, but since, at constant density, we find that the addition of Si increases both V_P and V_S , we believe that it will be very difficult to obtain a simultaneous match of the properties of any such hcp-Fe–Si alloy to the observed inner-core density and wave velocities. The addition of Si to hcp-Fe did not significantly change the anisotropy in V_P in this system. Our conclusions, therefore, differ from those of Antonangeli et al. (2010) and Mao et al. (2012) who have suggested, on the basis of extrapolations of experimental measurements of sound velocity as a function of density, that inner-core density and P-wave velocity can be matched simultaneously by the properties of a hexagonal-close-packed (hcp) Fe–Si or Fe–Ni–Si alloy. This apparent difference in conclusions has been readily explained by reference to the work of Antonangeli and Ohtani (2015); in one case (Antonangeli et al., 2010) an incorrect velocity–density relationship for pure hcp-Fe was assumed, and in the other case (Mao et al., 2012) there are doubts as to the experimental methodology used and large uncertainties inherent in the extrapolation of these experimental results to inner-core conditions.

Acknowledgements

This work was supported by Natural Environment Research Council grant NE/H003975/1 awarded to LV. Calculations were performed in the HECTOR & ARCHER supercomputer facilities.

References

- Alfè, D., Gillan, M.J., Price, G.D., 2007. Temperature and composition of the Earth's core. *Contemp. Phys.* 48, 63–80.
- Alfè, D., 2009. Temperature of the inner-core boundary of the Earth: melting of iron at high pressure from first-principles coexistence simulations. *Phys. Rev. B* 79, 060101.
- Antonangeli, D., Siebert, J., Badro, J., Farber, D.L., Fiquet, G., Morard, G., Ryerson, F.J., 2010. Composition of the Earth's inner core from high-pressure sound velocity measurements in Fe–Ni–Si alloys. *Earth Planet. Sci. Lett.* 295, 292–296.
- Antonangeli, D., Ohtani, E., 2015. Sound velocity of hcp-Fe at high pressure: experimental constraints, extrapolations and comparison with seismic models. *Prog. Earth Planet. Sci.* 2, 3. <http://dx.doi.org/10.1186/s40645-015-0034-9>.
- Asanuma, H., Ohtani, E., Sakai, T., Terasaki, H., Kamada, S., Hirao, N., Sata, N., Ohishi, Y., 2008. Phase relations of Fe–Si alloy up to core conditions: implications for the Earth inner core. *Geophys. Res. Lett.* 35, L12307.
- Asanuma, H., Ohtani, E., Sakai, T., Terasaki, H., Kamada, S., Hirao, N., Ohishi, Y., 2011. Static compression of Fe_{0.83}Ni_{0.09}Si_{0.08} alloy to 374 GPa and Fe_{0.93}Si_{0.07} alloy

- to 252 GPa: implications for the Earth's inner core. *Earth Planet. Sci. Lett.* 310, 113–118.
- Badro, J., Côté, A.S., Brodholt, J.P., 2014. A seismologically consistent compositional model of Earth's core. *Proc. Natl. Acad. Sci. USA* 111, 7542–7545.
- Badro, J., Fiquet, G., Guyot, F., Gregoryanz, E., Occelli, F., Antonangeli, D., d'Astuto, M., 2007. Effect of light elements on the sound velocities in solid iron: implications for the composition of Earth's core. *Earth Planet. Sci. Lett.* 254, 233–238.
- Birch, F., 1952. Elasticity and constitution of the Earth's interior. *J. Geophys. Res.* 57, 227–286.
- Blöchl, P.E., 1994. Projector augmented-wave method. *Phys. Rev. B* 50, 17953–17979.
- Côté, A.S., Vočadlo, L., Brodholt, J.P., 2008. The effect of silicon impurities on the phase diagram of iron and possible implications for the Earth's core structure. *J. Phys. Chem. Solids* 69, 2177–2181.
- Côté, A.S., Vočadlo, L., Dobson, D.P., Alfè, D., Brodholt, J.P., 2010. *Ab initio* lattice dynamics calculations on the combined effect of temperature and silicon on the stability of different iron phases in the Earth's inner core. *Phys. Earth Planet. Inter.* 178, 2–7.
- Davies, R.H., Dinsdale, A.T., Gisby, J.A., Robinson, J.A.J., Martin, S.M., 2002. MT-DATA – thermodynamic and phase equilibrium software from the national physical laboratory. *Calphad* 26 (2), 229–271. [http://dx.doi.org/10.1016/S0364-5916\(02\)00036-6](http://dx.doi.org/10.1016/S0364-5916(02)00036-6).
- Deng, L., Fei, Y., Liu, X., Gong, Z., Shahar, A., 2013. Effect of carbon, sulphur and silicon on iron melting at high pressure: implications for composition and evolution of the planetary terrestrial cores. *Geochim. Cosmochim. Acta* 114, 220–233.
- Dziewonski, A.M., Anderson, D.L., 1981. Preliminary reference Earth model. *Phys. Earth Planet. Inter.* 25, 297–356.
- Fischer, R.A., Campbell, A.J., Caracas, R., Reaman, D.M., Dera, P., Prakapenka, V.B., 2012. Equation of state and phase diagram of Fe–¹⁶Si as a candidate component of Earth's core. *Earth Planet. Sci. Lett.* 357–358, 268–276.
- Fischer, R.A., Campbell, A.J., Reaman, D.M., Miller, N.A., Heinz, D.L., Dera, P., Prakapenka, V.B., 2013. Phase relations in the Fe–FeSi system at high pressure and temperatures. *Earth Planet. Sci. Lett.* 373, 54–64.
- Fischer, R.A., Campbell, A.J., Caracas, R., Reaman, D.M., Heinz, D.L., Prakapenka, V.B., 2014. Equations of state in the Fe–FeSi system at high pressures and temperatures. *J. Geophys. Res.* 119, 2810–2827.
- Hernández, E., 2001. Metric-tensor flexible-cell algorithm for isothermal isobaric molecular dynamics simulations. *J. Chem. Phys.* 115, 10282–10290.
- Hirao, N., Ohtani, E., Kondo, T., Kikegawa, T., 2004. Equation of state of iron–silicon alloys to megabar pressure. *Phys. Chem. Miner.* 31, 329–336.
- Hirose, K., Labrosse, S., Hernlund, J., 2013. Composition and state of the core. *Annu. Rev. Earth Planet. Sci.* 41, 657–691.
- Kresse, G., Hafner, J., 1993a. *Ab initio* molecular dynamics for liquid metals. *Phys. Rev. B* 47, 558–561.
- Kresse, G., Hafner, J., 1993b. *Ab initio* molecular dynamics for open-shell transition metals. *Phys. Rev. B* 48, 13115–13118.
- Kresse, G., Hafner, J., 1994. *Ab initio* molecular-dynamics simulation of the liquid-metal–amorphous-semiconductor transition in germanium. *Phys. Rev. B* 49, 14251–14269.
- Kresse, G., Joubert, D., 1999. From ultrasoft pseudopotentials to the projector augmented-wave method. *Phys. Rev. B* 59, 1758–1775.
- Kuwayama, Y., Sawai, T., Hirose, K., Stat, N., Ohishi, Y., 2009. Phase relations of iron–silicon alloys at high pressure and high temperature. *Phys. Chem. Miner.* 36, 511–518.
- Labrosse, S., 2014. Thermal and compositional stratification of the inner core. *C. R. Géosci.* 346, 119–129.
- Lin, J.-F., Campbell, J., Heinz, D.L., 2003a. Static compression of iron–silicon alloys: implications for silicon in the Earth's core. *J. Geophys. Res.* 108, 2045.
- Lin, J.-F., Struzhkin, V.V., Sturhahn, W., Huang, E., Zhao, J., Hu, Y.H., Alp, E.E., Mao, H.-K., Boctor, N., Hemley, J., 2003b. Sound velocities of iron–nickel and iron–silicon alloys at high pressures. *Geophys. Res. Lett.* 30, 2112.
- Mainprice, D., 1990. An efficient Fortran program to calculate seismic anisotropy from the lattice preferred orientation of minerals. *Comput. Geosci.* 16, 385–393. <http://www.gm.univ-montp2.fr/PERSO/mainprice/>.
- Mao, Z., Lin, J.-F., Liu, J., Alatas, A., Gao, L., Zhao, J., Mao, H.-K., 2012. Sound velocities of Fe and Fe–Si alloy in the Earth's core. *Proc. Natl. Acad. Sci. USA* 109, 10239–10244.
- Martorell, B., Vočadlo, L., Brodholt, J., Wood, I.G., 2013a. Strong pre-melting effect in the elastic properties of hcp-Fe under inner-core conditions. *Science* 342, 466–468.
- Martorell, B., Brodholt, J., Wood, I.G., Vočadlo, L., 2013b. The effect of nickel on the properties of iron at the conditions of Earth's inner core: *ab initio* calculations of seismic wave velocities of Fe–Ni alloys. *Earth Planet. Sci. Lett.* 365, 143–151.
- Martorell, B., Vočadlo, L., Brodholt, J., Wood, I.G., 2015. The elastic properties of fcc-Fe and fcc-FeNi alloys at inner-core conditions up to the fcc–hcp phase transition. *Geophys. J. Int.* 202, 94–101.
- Morard, G., Bouchet, J., Valencia, D., Mazevet, S., Guyot, F., 2011. The melting curve of iron at extreme pressures: implications for planetary cores. *High Energy Density Phys.* 7, 141–144.
- Nadal, M.-H., Hubert, C., Ultra, R., 2009. High temperature shear modulus determination using a laser-ultrasonic surface acoustic-wave device. *J. Appl. Phys.* 106, 024906.
- Nadal, M.-H., Le Poac, P., 2003. Continuous model for the shear modulus as a function of pressure and temperature up to the melting point: analysis and ultrasonic validation. *J. Appl. Phys.* 93, 2472–2480.
- Nguyen, J.H., Akin, M.C., Chau, R., Fratanduono, D.E., Ambrose, W.P., Fat'yanov, O.V., Asimov, P.D., Holmes, N.C., 2014. Molybdenum sound velocity and shear modulus softening under shock compression. *Phys. Rev. B* 89, 17109.
- Perdew, J.P., Wang, Y., 1992. Accurate and simple analytic representation of the electron–gas correlation energy. *Phys. Rev. B* 45, 13244–13249.
- Sakamaki, T., et al., 2016. Constraints on Earth's inner core composition inferred from measurements of the sound velocity of hcp-iron in extreme conditions. *Sci. Adv.* 2, e1500802.
- Sha, X., Cohen, R.E., 2010. Elastic isotropy of ϵ -Fe under Earth's core conditions. *Geophys. Res. Lett.* 37, L10302.
- Souriau, A., 2007. Deep Earth structure—the Earth's cores. In: Schubert, G. (Ed.), *Treatise on Geophysics*, Vol. 1: Seismology and the Structure of the Earth. Elsevier, Amsterdam, pp. 655–693.
- Tkalčić, H., 2015. Complex inner core of the Earth: the last frontier of global seismology. *Rev. Geophys.* 53, 59–94.
- Tsuchiya, T., Fujibuchi, M., 2009. Effects of Si on the elastic property of Fe at Earth's inner core pressures: first principles study. *Phys. Earth Planet. Inter.* 174, 212–219.
- Vočadlo, L., Alfè, D., Gillan, M.J., Price, G.D., 2003. The properties of iron under core conditions from first principles calculations. *Phys. Earth Planet. Inter.* 140, 101–125.
- Vočadlo, L., 2007. *Ab initio* calculations of the elasticity of iron alloys at inner core conditions: evidence for a partially molten inner core? *Earth Planet. Sci. Lett.* 254, 227–232.
- Vočadlo, L., Dobson, D., Wood, I.G., 2009. *Ab initio* calculations of the elasticity of hcp-Fe as a function of temperature at inner-core pressure. *Earth Planet. Sci. Lett.* 288, 534–538.
- Wang, T., Song, X., Xia, H.H., 2015. Equatorial anisotropy in the inner part of Earth's inner core from autocorrelation of earthquake coda. *Nat. Geosci.* 8, 224–227.
- Yunker, M.L., Van Orman, J.A., 2007. Interdiffusion of solid iron and nickel at high pressure. *Earth Planet. Sci. Lett.* 254, 203–213.